

High-efficiency, high-average-power, CW Yb:YAG zigzag slab master oscillator power amplifier at room temperature

XIAOMING CHEN,^{1,2} LIU XU,^{1,2,*} HAO HU,^{1,2} TANGJIAN ZHOU,^{1,2} YINHONG SUN,^{1,2} HAO JIANG,^{1,2,4} JUN LEI,^{1,2} WENQIANG LV,^{1,2} HUA SU,^{2,3} YONG SHI,^{1,2} MI LI,^{1,2} YINGCHEN WU,^{1,2} ZHENYU YAO,^{1,2} NA ZHAO,^{1,2} XIAOXIAO XU,^{1,2} QINGSONG GAO,^{1,2} XIAOJUN WANG,^{1,2,3} AND CHUN TANG^{1,2}

¹Institute of Applied Electronics, China Academy of Engineering Physics, Mianyang, Sichuan 621900, China

²Key Laboratory of Science and Technology on High Energy Laser, China Academy of Engineering Physics, Mianyang, Sichuan 621900, China

³Institute of Applied Physics and Computational Mathematics, Beijing 100088, China

⁴Graduate School, China Academy of Engineering Physics, Beijing 100088, China

*chenxiaomingzs@163.com

Abstract: We demonstrate a high-efficiency, high-average-power, CW master oscillator power amplifier based on a conduction-cooled, end-pumped Yb:YAG slab architecture at room temperature (RT). Firstly, the CW amplification property is theoretically analyzed based on the kinetics model for Yb:YAG. To realize high-efficiency laser amplification extraction for RT Yb:YAG, not only intense pump but also a high-power seed laser is of great importance. Experimentally, a composite Yb:YAG crystal slab with three doped and two undoped segments symmetrically is employed as the gain medium, which is end-pumped by two high-power, 940-nm diode lasers. A high-power, narrow-spectral-width, 1030-nm fiber seed laser then double passes the composite slab to realize efficient power amplification. For 0.8-kW seed input, maximum output power of 3.54 kW is obtained at 6.7 kW of pump power, with the optical conversion efficiency of 41% and the highest slope efficiency of 59%. To the best of our knowledge, this is the highest power and efficiency reported for Yb:YAG lasing at RT except thin-disk lasers.

© 2016 Optical Society of America

OCIS codes: (140.3480) Lasers, diode-pumped; (140.3580) Lasers, solid-state; (140.3615) Lasers, ytterbium; (140.3280) Laser amplifiers.

References and links

1. W. F. Krupke, "Ytterbium solid-state lasers. The first decade," *IEEE J. Sel. Top. Quantum Electron.* **6**(6), 1287–1296 (2000).
2. D. S. Sumida, H. W. Bruesselbach, R. W. Byren, M. S. Mangir, and R. Reeder, "High-power Yb:YAG rod oscillators and amplifiers," *Proc. SPIE* **3265**, 100–105 (1998).
3. H. Bruesselbach and D. S. Sumida, "A 2.65-kW Yb:YAG single-rod laser," *IEEE J. Sel. Top. Quantum Electron.* **11**(3), 600–603 (2005).
4. A. Giesen and J. Speiser, "Fifteen years of work on thin-disk lasers: results and scaling laws," *IEEE J. Sel. Top. Quantum Electron.* **13**(3), 598–609 (2007).
5. G. D. Goodno, S. Palese, J. Harkenrider, and H. Injeyan, "Yb:YAG power oscillator with high brightness and linear polarization," *Opt. Lett.* **26**(21), 1672–1674 (2001).
6. D. C. Brown, "The promise of cryogenic solid-state lasers," *IEEE J. Sel. Top. Quantum Electron.* **11**(3), 587–599 (2005).
7. T. Y. Fan, D. J. Ripin, R. L. Aggarwal, J. R. Ochoa, B. Chann, M. Tilleman, and J. Spitzberg, "Cryogenic Yb³⁺-doped solid-state lasers," *IEEE J. Sel. Top. Quantum Electron.* **13**(3), 448–459 (2007).
8. S. Redmond, S. Mcnaught, J. Zamel, L. Iwaki, S. Bammert, R. Simpson, S. B. Weiss, J. Szot, B. Flegel, and T. Lee, "15 kW near-diffraction-limited single-frequency Nd:YAG laser," in *Conference on Lasers and Electro-Optics* (2007), pp. 1–2.

9. G. D. Goodno, H. Komine, S. J. McNaught, S. B. Weiss, S. Redmond, W. Long, R. Simpson, E. C. Cheung, D. Howland, P. Epp, M. Weber, M. McClellan, J. Sollee, and H. Injeyan, "Coherent combination of high-power, zigzag slab lasers," *Opt. Lett.* **31**(9), 1247–1249 (2006).
10. R. Wilhelm, D. Freiburg, M. Frede, D. Kracht, and C. Fallnich, "Design and comparison of composite rod crystals for power scaling of diode end-pumped Nd:YAG lasers," *Opt. Express* **17**(10), 8229–8236 (2009).
11. Y. J. Huang and Y. F. Chen, "High-power diode-end-pumped laser with multi-segmented Nd-doped yttrium vanadate," *Opt. Express* **21**(13), 16063–16068 (2013).
12. D. C. Brown and V. A. Vitali, "Yb:YAG kinetics model including saturation and power conservation," *IEEE J. Quantum Electron.* **47**(1), 3–12 (2011).
13. G. L. Bourdet, "Theoretical investigation of quasi-three-level longitudinally pumped continuous wave lasers," *Appl. Opt.* **39**(6), 966–971 (2000).
14. C. Lim and Y. Izawa, "Modeling of end-pumped CW quasi-three-level lasers," *IEEE J. Quantum Electron.* **38**(3), 306–311 (2002).
15. J. K. Brasseur, A. K. Abeeluck, A. R. Awtry, L. S. Meng, K. E. Shortoff, N. J. Miller, R. K. Hampton, M. H. Cuchiara, and D. K. Neumann, "2.3-kW continuous operation cryogenic Yb:YAG laser," *Proc. SPIE* **6952**, 69520L (2008).
16. M. Ganija, D. J. Ottaway, P. J. Veitch, and J. Munch, "Cryogenic, conduction cooled, end pumped, zigzag slab laser, suitable for power scaling," in *Conference on Lasers and Electro-Optics*, CM3D.7, (2012).
17. S. Matsubara, T. Ueda, T. Takamido, and S. Kawato, "Nearly quantum-efficiency limited oscillation of Yb:YAG laser at room temperature," in *Conference on Lasers and Electro-Optics* (2005), pp. 325–327.
18. J. Dong, A. Shirakawa, K. I. Ueda, and A. A. Kaminskii, "Effect of ytterbium concentration on CW Yb:YAG microchip laser performance at ambient temperature – Part II: Theoretical modeling," *Appl. Phys. B* **89**(2-3), 367–376 (2007).
19. H. Yoshioka, S. Nakamura, Y. Matsubara, T. Ogawa, and S. Wada, "Efficient tunable diode-pumped Yb:YAG ceramic laser," in *Conference on Quantum Electronics and Laser Science* (2008), pp. 1–2.

1. Introduction

Because of its low quantum defect and broad absorption band, quasi-three-level Yb:YAG has been studied extensively to develop high-efficiency, high-average-power, diode-pumped lasers [1–5]. However, it is a great challenge to overcome the thermal population (~5%) of the lower lasing level at room temperature (RT), due to the proximity of the lower lasing level to the ground state [6,7]. To realize high-efficiency, high-average-power Yb:YAG lasers at RT, intense pumping [1–5] is required, which becomes possible owing to the development of high-efficiency and high-brightness diode pumps.

To date, several architectures have been demonstrated for RT high power and efficiency Yb:YAG laser system, including the rod [3], the thin-disk [4] and the zigzag slab [5] structure etc. In 2005, H. Bruesselbach and D. S. Sumida [3] reported a CW average-output-power of 2.65 kW from a single Yb:YAG laser rod pumped with 9 kW from 940-nm laser diodes with the optical conversion efficiency of 28%. However, high-power rod lasers with good beam quality are limited by seriously thermal effects. In 2007, the output power of one single thin-disk has been increased to more than 5.3 kW with the maximum optical efficiency of more than 65% [4]. The face cooling of thin-disk lasers minimizes the transversal temperature gradient and the phase distortions transversal to the direction of the beam propagation. Therefore, it seems as the highest power and efficiency scheme for high-beam-quality Yb:YAG operation at RT. Nevertheless, the pump structures are usually quite complicated to reflect the pump power to be absorbed well. Different from the rod and thin-disk structures, zigzag slabs have the potential to provide high beam quality because zigzag propagation by means of total internal reflections (TIR) eliminates thermo-optic path difference and birefringence over the entire beam area [5,8,9]. In addition, a conduction-cooled, end-pumped slab (CCEPS) decouples the slab absorption length from the two large cooling faces of the slab, thus providing intense pumping and efficient cooling, which is important in quasi-three-level lasers. In 2001, G. D. Goodno et al [5] demonstrated a CCEPS Yb:YAG laser at RT, realizing 415 W of CW power and 30% optical conversion efficiency. The 940-nm pump light was concentrated to 20 kW/cm² at the 1 at.%-doped slab, and more intense pump was limited by thermal gradient and accompanied mechanical tensile stress inside the gain medium. Recently, it was shown that the crystal composed of multiple segments [10,11] with different doping concentrations in the pump direction can flatten the longitudinal temperature

and stress distributions to permit a higher pump power before the thermal fracture occurs, which is favorable for developing RT high power and efficiency Yb:YAG lasers.

In this paper, we originally present a high-efficiency, high-average-power, CW master oscillator power amplifier (MOPA) at RT based on a CCEPS Yb:YAG architecture. Firstly, the CW amplification property is theoretically analyzed based on the kinetics model for Yb:YAG. Different from a laser oscillator, to realize high-efficiency laser amplification extraction for RT Yb:YAG, not only intense pump but also a high-power seed laser is important. Experimentally, a composite Yb:YAG crystal slab with three doped and two undoped segments symmetrically is employed as the gain medium, which is end-pumped by two high-power, 940-nm diode lasers. A high-power, narrow-spectral-width, 1030-nm fiber seed laser then double passes the composite slab to realize efficient power amplification. Finally, when the input seed power is 0.8 kW and the pump power 6.7 kW, maximum output power of 3.54 kW and 41% optical conversion efficiency are demonstrated.

2. Theoretical analysis

In this section, the CW amplification property is theoretically analyzed based on the kinetics model for Yb:YAG [12–14], which is helpful for the optimization of the following experimental parameters.

For Yb:YAG pumped at 940 nm and lasing at 1030 nm, the gain coefficient in stationary CW condition is given by [12]

$$g = \sigma_L (f_{11}n_1 - f_{03}n_0) = \sigma_L n_d \frac{\frac{I_p}{I_p^S} (f_{01}f_{11} - f_{03}f_{12}) - f_{03}}{1 + \frac{I_p}{I_p^S} (f_{01} + f_{12}) + \frac{I_L}{I_L^S} (f_{03} + f_{11})}. \quad (1)$$

The denotations adopted here are all the same as those defined in [12], where σ_L is the effective stimulated-emission cross section, f_{ij} are the Boltzmann occupation factors for the upper ${}^2F_{5/2}$ and lower ${}^2F_{7/2}$ manifolds, and n_1 and n_0 are ion number densities of the upper and lower manifolds respectively, n_d is the Yb doping density, and I_p and I_L are the pump and laser intensities, I_p^S and I_L^S are the pump and laser saturation intensities, respectively. Then, as to a laser amplifier, the power extraction efficiency can be defined as [12]

$$\eta_{ex} = \frac{P_{ex}}{P_{ST}} = \frac{P_{out} - P_{in}}{P_{ST}} = \frac{1 - \frac{f_{03}}{f_{01}f_{11} - f_{03}f_{12}} \frac{I_p^S}{I_p}}{1 + \frac{f_{01}}{f_{01}f_{11} - f_{03}f_{12}} \frac{I_L^S}{I_L}}, \quad (2)$$

where P_{ex} is the laser power extracted from a volume element, P_{in} and P_{out} are the input and output power from the same volume element, and P_{ST} is power stored in the upper laser manifold. The extraction efficiency is a function of both I_L/I_L^S and I_p/I_p^S , and also temperature-dependent Boltzmann occupation factors. In order to get net positive gain and extraction efficiency > 0 , the ratio I_p/I_p^S must satisfy

$$\frac{I_p}{I_p^S} > \frac{f_{03}}{f_{01}f_{11} - f_{03}f_{12}}, \quad (3)$$

which is primarily determined by the thermal population of the lower lasing level, i.e. material temperature [12].

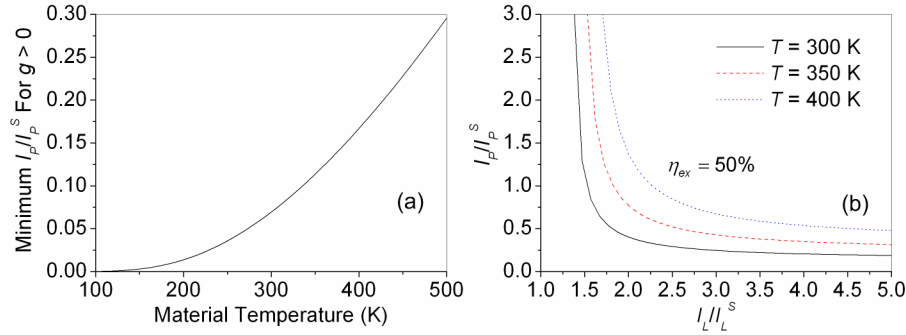


Fig. 1. (a) Calculated minimum I_p/I_p^S for $g > 0$ as a function of material temperature and (b) relationship between I_L/I_L^S and I_p/I_p^S for $\eta_{ex} = 50\%$ when $T = 300, 350$ and 400 K respectively.

Figure 1(a) shows the calculated minimum I_p/I_p^S for getting net positive gain as a function of material temperature (T), with T varying from 100 to 500 K. At low temperature, the lower lasing level becomes thermally depopulated, thus resulting in a low pump threshold [6,7]. For T lower than 100 K, Yb:YAG can be regarded as a four-level laser system. Nevertheless, much higher pump threshold is required with the increasing of T , and now Yb:YAG should be treated as a quasi-three-level laser system. Figure 1(b) shows the relationship between I_L/I_L^S and I_p/I_p^S for $\eta_{ex} = 50\%$ when $T = 300, 350$ and 400 K respectively. Not only high pump intensity but also an intense seed laser is needed to obtain an efficient amplification extraction at RT or above. In addition, higher pump and laser intensities are needed with the increasing of T . For Yb:YAG, $I_p^S \approx 29$ kW/cm² and $I_L^S \approx 10$ kW/cm². Therefore, as to $T = 350$ K, the minimum pump intensity needed for $g > 0$ is about 3.3 kW/cm², and $I_p > 9$ kW/cm² and $I_L > 15$ kW/cm² are required for $\eta_{ex} = 50\%$.

Based on the above analysis, cryogenic cooling is a potential way to develop low-threshold and high-efficiency Yb:YAG laser outputs [6,7,15,16]. However, both high pump and laser intensities are needed to realize high-efficiency lasing at RT. Then, for a laser oscillator, the internal laser intensity is quite high thanks to the feed back by cavity mirrors, and thus only intense pumping is needed to obtain high-efficiency laser output. Highly efficient operation has been demonstrated based on Yb:YAG microchip lasers at RT [17–19]. S. Matsubara et al [17] reported nearly quantum-efficiency limited oscillation of 1-mm thick Yb:YAG laser. The maximum pump intensity was about 0.3 MW/cm² and the internal laser intensity ~ 4.5 MW/cm², far beyond the saturation intensity of Yb:YAG. Consequently, maximum slope efficiency of 140% and optical efficiency of 89% were achieved at an absorbed pump power of 850 mW. Different from the laser oscillators, the seed laser usually passes several times or even just once through the gain medium as to a laser amplifier. Hence, to realize high-efficiency laser amplification extraction for RT Yb:YAG, not only intense pump but also a high-power seed laser is of great importance.

3. Experimental setup

The experimental arrangement for exploring the laser performance of the CCEPS Yb:YAG MOPA is schematically depicted in Fig. 2(a). A composite Yb:YAG crystal slab with three doped and two un-doped segments symmetrically is employed as the gain medium. The dimensions of the composite slab are 82 mm (z) \times 10 mm (y) \times 1.8 mm (x) (length \times width \times thickness). The central 32-mm length of the slab is 1 at.-%-doped Yb:YAG, diffusion-bonded with two 18-mm long, 0.6 at.-%-doped Yb:YAG and then 7-mm long, un-doped YAG end caps. The two end faces of the slab are 45°-cut and anti-reflection coated at 1030 nm. The two sides of the slab are roughened to suppress the amplified spontaneous emission (ASE) and parasitic oscillation. To handle the large heat loads with minimal temperature rise, we place water-cooled micro-channel copper coolers in thermal contact with the slab TIR faces. A 3-

μm thick SiO_2 evanescent wave coating is used to protect the TIR faces. The thickness of the SiO_2 coating is tailored to provide a transmission maximum at the 940-nm pump wavelength. The slab is end-pumped by two 4-kW diode laser arrays, with an emitting area of 10 mm (y) \times 54 mm (x). The pump light is shaped by two slow-axis cylindrical lenses ($f_{py1} = 100$ mm and $f_{py2} = 50$ mm) and focused by another fast-axis cylindrical lens ($f_{px} = 140$ mm), and injected via TIR from the 45° end faces. To avoid the leakage pump power from one end hit and damage the other pump diodes, two 45° -polarizers (P_p) and a $\lambda/2$ wave-plate are used in the pump coupling system. The un-absorbed pump power is leaked out from the 45° -polarizers and absorbed by two water-cooled Cu-absorbers. The pump coupling efficiency is about 90% and the diameter of the pump beam at the input faces is about 5-mm width. Maximum pump intensity of 40 kW/cm² is available. Next, a homemade high-power, narrow line-width fiber seed laser is used as the extracting signal beam of the MOPA. The maximum output power of the fiber laser is about 1 kW, with the central wavelength of 1030.03 nm and the line width of 0.08 nm, and the beam quality of $M^2 < 2$. The central wavelength of the seed laser coincides well with the peak-emission wavelength of Yb:YAG and the line width is much narrower than the emission line-width of Yb:YAG (~ 6 nm) [1], which is favorable for laser amplification. The diameter of the signal beam is about 6 mm (y) \times 1.8 mm (x) at the first input face of the slab after passing through an optical isolator and a beam shaping system. The beam shaping system is comprised of four cylindrical lenses ($f_{sy1} = 172$ mm, $f_{sy2} = 208$ mm, $f_{sx1} = 280$ mm and $f_{sx2} = 100$ mm, with $f_{sy1} + f_{sy2} = f_{sx1} + f_{sx2}$). The signal beam is shaped in the x and y directions respectively, and the image planes are superposed at the first input face of the slab. Whereafter, the signal beam passes twice through the slab via zigzag path with the incidence angles of 45.3° and 35.7° . The output beam after the first pass is $4f$ imaged before the second pass with the help of two spherical lenses ($f_s = 360$ mm) and high-reflectivity (HR) coating mirrors.

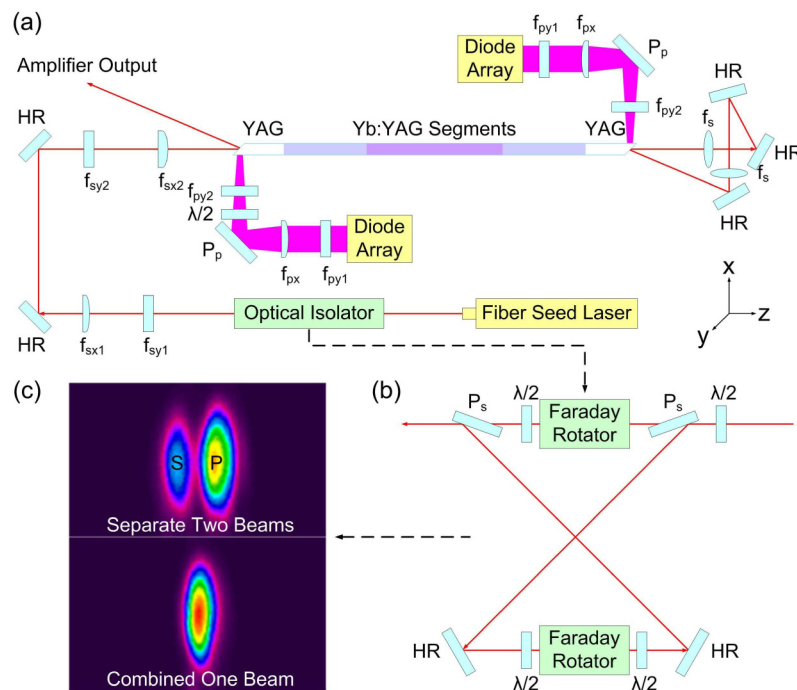


Fig. 2. (a) Schematic of the experimental setup, (b) the optical isolator and (c) the far-field beam pattern of the signal beam after the optical isolator and beam shaping system.

It should be pointed out that the output beam of the fiber seed laser is non-polarized. It is difficult to implement optical isolation of such a high-power, non-polarized beam. Figure 2(b) shows the configuration of the optical isolator, including two Faraday isolators and the polarization beam combination system. The non-polarized signal beam is separated to P and S polarized components by a quartz polarizer (P_s). And the P and S polarized components are combined together newly at another quartz polarizer at last. The far-field beam pattern of the signal beam after the optical isolator and beam shaping system was measured by a CCD camera, as shown in Fig. 2(c). The upper figure shows the separate P and S polarized components, and the lower one shows the well-combined beam. Finally, maximum signal power of 0.8 kW is available at the input face of the slab, with the total propagation efficiency of 80%.

4. Results and discussion

In the experiments, the coolant temperature for the slab was set to 15 °C and the pump absorption efficiency was about 95%. The pump beam and the signal beam were aligned to overlap in the middle region of the slab.

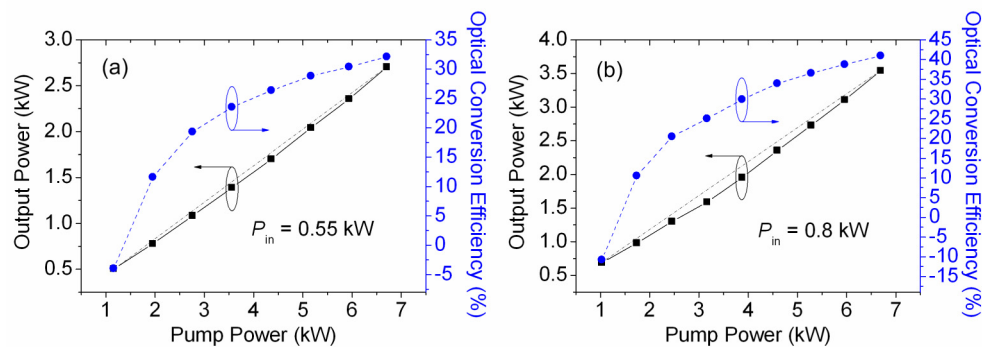


Fig. 3. Amplifier output power and optical conversion efficiency as a function of pump power when the input signal power is (a) 0.55 kW and (b) 0.8 kW, respectively.

Figure 3 shows the amplifier output power and optical conversion efficiency when the input signal power is 0.55 and 0.8 kW, respectively. As $P_{in} = 0.55$ kW, the signal beam power is reduced to 0.2 kW after passing twice through the un-pumped slab. This is caused by the reabsorption of the Yb:YAG at the lasing wavelength, due to thermal population of the lower lasing level. Until the pump power is up to 1.36 kW, the signal beam gets a net positive amplification. Then, the output power increases almost linearly relative to the pump power. Meanwhile, slight increase of the slope efficiency is observed with the increase of the pump power, which can be explained by Eq. (2). Though the pump-induced temperature rising is harmful for efficient amplification, the enhancement by the increase of both pump and signal intensities brings about the increase of the extraction efficiency. Finally, 2.7 kW of power output at 1030 nm is obtained at 6.7 kW of pump power, with the optical conversion efficiency of 32% and the highest slope efficiency of 45%. Higher pump was limited by the temperature rise of the rough sides of the slab, about 90 °C at the pump power of 6.7 kW. The amplifier performance for $P_{in} = 0.8$ kW is similar to that of $P_{in} = 0.55$ kW. Maximum output power of 3.54 kW is obtained at 6.7 kW of pump power, with the optical conversion efficiency of 41% and the highest slope efficiency of 59%, which is the highest power and efficiency reported for Yb:YAG lasing at RT except thin-disk lasers [4]. The increase in optical efficiency of about 9% relative to that of $P_{in} = 0.55$ kW is much higher than the theoretically calculated value (based on Eq. (2)) of 2%, which can be explained by the stronger ASE-suppression and lower temperature for higher signal input of $P_{in} = 0.8$ kW. It

was observed that the temperature rise of the slab reduced from 90 to 63 °C at 6.7 kW of pump power.

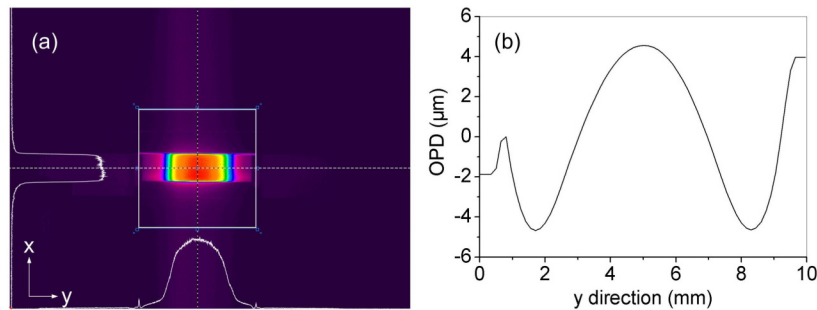


Fig. 4. (a) The fluorescence distribution induced by the pump beam and (b) the optical path difference information of the slab along the y direction at the pump power of 2.5 kW (without signal inputting).

It should be mentioned that the output beam was quite unstable with the increasing of the pump power under signal inputting. This is caused mainly by two aspects. First, obvious transversal mode-hop of the fiber seed laser was observed during the increasing of the signal power. Secondly, there exists a strong focus in the middle region of the slab along the width (y) direction, mainly resulted by the super-Gaussian intensity distribution of the pump beam. The fluorescence distribution induced by the pump beam is shown in Fig. 4(a), which truly indicates the intensity distribution property of the pump beam in the slab. The optical path difference (OPD) information of the slab was measured by a Shack-Hartman wavefront sensor and a He-Ne laser at the pump power of 2.5 kW (without signal inputting), as shown in Fig. 4(b). Except for a strong focus in the middle region of the slab, the wavefront at the edges is poor due to the temperature rise of the rough sides of the slab. The poor wavefront is unfavorable for the overlapping of the pump and signal beams, and thus partly affects the power extraction of the amplifier.

5. Conclusion

In summary, a high-efficiency, high-average-power output is demonstrated based on a CCEPS Yb:YAG MOPA at RT. Theoretically, the CW amplification property is analyzed based on the kinetics model for Yb:YAG. Both intense pump and seed are needed to realize high-efficiency laser amplification extraction for RT Yb:YAG. Experimentally, under 0.8-kW signal input, maximum output power of 3.54 kW is obtained at 6.7 kW of pump power, with the optical conversion efficiency of 41% and the highest slope efficiency of 59%. Higher efficiency may be realized if more intense pumping and signal extracting are available. Furthermore, increasing the slab width and pump power while maintaining the same power density and thermal loads should provide straightforward power scaling to tens of kilowatt level. However, there are still many problems to be solved in our experiments, including the improvement of the transversal mode-stability of the 1030-nm fiber seed laser, the optimization of the pump uniformity and the design of the slab sides and so on, which will be researched in our future work.

Funding

Foundation of Key Laboratory of Science and Technology on High Energy Laser, China Academy of Engineering Physics (HEL 201X-04); Special Fund of Innovation of China Academy of Engineering Physics (CXZX-100X-03).